VIP Asymmetric Synthesis Very Important Paper

How to cite: *Angew. Chem. Int. Ed.* **2021**, *60*, 19428–19434
International Edition: doi.org/10.1002/anie.202107267
German Edition: doi.org/10.1002/ange.202107267

Site- and Enantioselective Iridium-Catalyzed Desymmetric Mono-Hydrogenation of 1,4-Dienes

*Haibo Wu, Hao Su, Erik J. Schulze, Bram B. C. Peters, Mark D. Nolan, Jianping Yang, Thishana Singh, Mårten S. G. Ahlquist, and Pher G. Andersson**

Abstract: *The control of site selectivity in asymmetric mono-hydrogenation of dienes or polyenes remains largely underdeveloped. Herein, we present a highly efficient desymmetrization of 1,4-dienes via iridium-catalyzed site- and enantioselective hydrogenation. This methodology demonstrates the first iridium-catalyzed hydrogenative desymmetriation of meso dienes and provides a concise approach to the installation of two vicinal stereogenic centers adjacent to an alkene. High isolated yields (up to 96%) and excellent diastereo- and enantioselectivities (up to 99:1 d.r. and 99% ee) were obtained for a series of divinyl carbinol and divinyl carbinamide substrates. DFT calculations reveal that an interaction between the hydroxy oxygen and the reacting hydride is responsible for the stereoselectivity of the desymmetrization of the divinyl carbinol. Based on the calculated energy profiles, a model that simulates product distribution over time was applied to show an intuitive kinetics of this process. The usefulness of the methodology was demonstrated by the synthesis of the key intermediates of natural products zaragozic acid A and (+)-invictolide.*

Introduction

Asymmetric hydrogenation of olefins has proved to be a powerful tool to produce enantiomerically enriched compounds on both laboratory and industrial scale.[1] Meanwhile, olefins are not only versatile precursors for a variety of organic transformations but also a common functional group ubiquitous in natural products, pharmaceuticals, and fine chemicals.[2] In this regard, the development of efficient methods to precisely control the site selectivity in the asymmetric mono-hydrogenation of dienes and polyenes is highly desirable for its further applications in organic synthesis (Figure 1).[3]

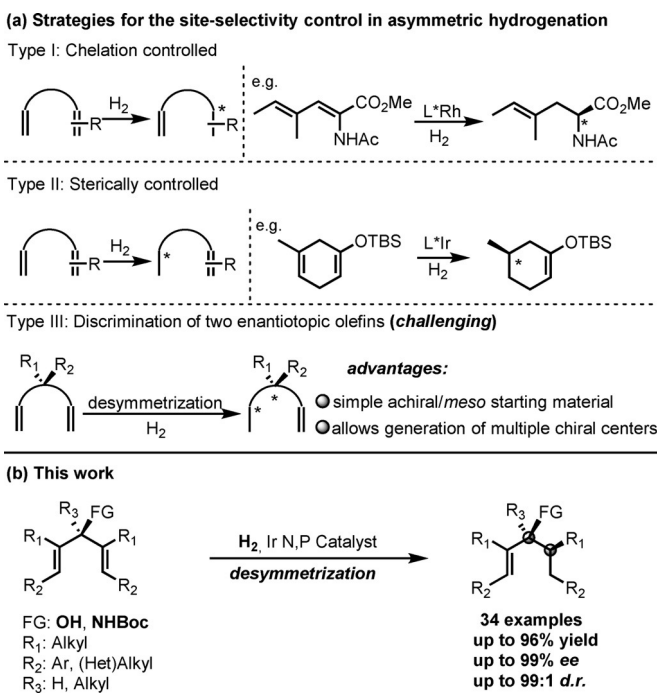

Figure 1. a) Strategies for site-selectivity control in asymmetric mono-hydrogenation of dienes. b) Ir-catalyzed hydrogenative desymmetrization of 1,4-dienes.

Despite significant progress in the field of enantioselective hydrogenation of different types of single olefins,[4] the discrimination between different olefins in the same molecule remains a challenging task. Classically, in order to differentiate one olefin from another, a chelating group such as alcohol,[3e] carboxylic acid,[3f] or amino acid[3g] needs to be present in the vicinity of the target alkene. This strategy was often used in Rh- and Ru-catalyzed hydrogenation of functionalized olefin substrates. In recent years, Pfaltz-type iridium N,P complexes have emerged as an efficient catalytic system for asymmetric hydrogenation of minimally function-

[*] H. Wu, E. J. Schulze, B. B. C. Peters, M. D. Nolan, J. Yang, Prof. P. G. Andersson
Department of Organic Chemistry
Stockholm University
10691 Stockholm (Sweden)
E-mail: pher.andersson@su.se
Dr. H. Su, Prof. M. S. G. Ahlquist
School of Biotechnology
KTH Royal Institute of Technology
10691 Stockholm (Sweden)
Dr. T. Singh, Prof. P. G. Andersson
School of Chemistry and Physics
University of Kwazulu-Natal
Private Bag X54001, Durban, 4000 (South Africa)
Supporting information and the ORCID identification number(s) for the author(s) of this article can be found under: https://doi.org/10.1002/anie.202107267.

alized olefins.[5] In this case, controlling the steric difference has become an alternative strategy for regioselective mono-hydrogenation of diene substrates without chelating groups.[3h] Nonetheless, the mentioned strategies require either the chelation or steric difference between the two olefins. Two enantiotopic olefins within the same molecule with identical chelating and steric environments makes the selective mono-hydrogenation even more challenging. This strategy known as desymmetrization has been widely applied in asymmetric synthesis,[6] however, the hydrogenative desymmetrization of dienes is so far underdeveloped.[6b] Initial work in this area was first reported by Brown in 2009, wherein moderate selectivities (up to 53% *ee*) were obtained for penta-1,4-dien-3-ol and its silyl ether by using Rh bisphosphine catalysts.[7] Later, Vidal-Ferran reported a novel Rh P–OP (phosphine–phosphite) complex-mediated hydrogenative desymmetrization of similar substrates with excellent selectivity (up to 92% *ee*).[8] Recently, the Zhang group described an elegant nickel-catalyzed hydrogenative desymmetrization of conjugated cyclohexadienones, providing an efficient access to all-carbon quaternary stereocenters.[9]

The products that could be derived from a selective mono-hydrogenation of a *meso* diene, chiral allylic alcohols, and amines bearing two vicinal stereocenters adjacent to the olefin are important structural units widely present in natural products and pharmaceuticals (Figure 2).[10] Conventional approaches for the synthesis of this type of complex moieties require multi-sequence steps and high cost of chiral reagents. The desymmetric hydrogenation of *meso* dienes would provide a straightforward strategy in the installation of two contiguous chiral centers next to the alkene.

Continuing our interest in practical regioselective asymmetric hydrogenations,[3h,11] we sought to develop a general hydrogenative desymmetrization of non-conjugated 1,4-dienes bearing different functionalities. Herein, we disclose a highly efficient desymmetrization of divinyl carbinols and divinyl carbinamines via iridium-catalyzed regio-, diastereo- and enantioselective hydrogenation. To the best of our knowledge, this method represents the first example of Ir-catalyzed hydrogenative desymmetrization of dienes. Moreover, the desymmetrization of N-containing achiral compounds via asymmetric hydrogenation is still rare.

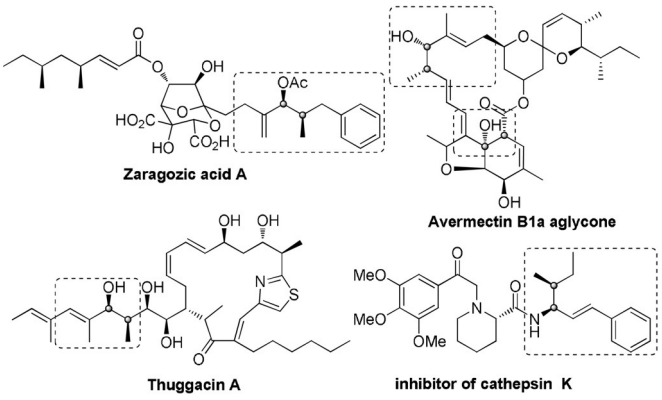

Figure 2. Selected examples of natural products and bioactive compounds containing an allylic alcohol or allylic amide bearing two contiguous chiral centers adjacent to an alkene.

Results and Discussion

Our initial investigation began with the attempted desymmetric hydrogenation of *meso* divinyl carbinol **1a**. Treatment of **1a** with an iridium N,P catalyst (**A**, 0.5 mol%) bearing an imidazole ligand and K_2CO_3 (10 mol%) as the additive in toluene at room temperature under 3 bar of hydrogen for 1 hour gave the desired mono-hydrogenated product **2a** in 89% NMR yield with 96:4 d.r. and 97% *ee* (Table 1, entry 1). Next, a series of Ir N,P catalysts were screened to evaluate the ligand effect (Table 1, entries 2–6). It was found that thiazole catalyst **C** and oxazoline catalyst **F** could give equally promising results as catalyst **A** in terms of diastereoselectivity

Table 1: Optimization of the reaction conditions.[a]

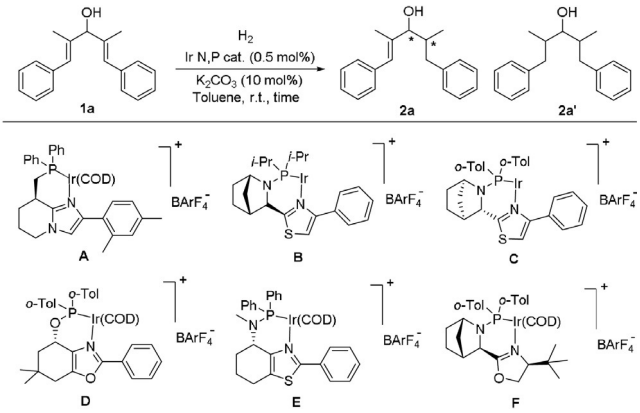

Entry	Cat.	*P*/*t*	Conv. [%][b]	**2a**/**2a′** [%][c]	**2a** d.r./*ee* [%][c]
1	**A**	3 bar/1 h	>99	89/11	96:4/97
2	**B**	3 bar/1 h	32	25/7	68:32/96
3	**C**	3 bar/1 h	>99	64/36	99:1/99
4	**D**	6 bar/1 h	27	25/2	69:31/99
5	**E**	6 bar/1 h	<5	N.D.[e]	N.D.[e]
6	**F**	3 bar/1 h	>99	82/18	93:7/99
7	**A**	3 bar/20 min	66	63/3	94:6/95
8[d]	**C**	1 bar/10 min	42	42/0	97:3/99
9	**C**	1 bar/10 min	>99	95/5	99:1/99

[a] Reaction conditions: **1a** (0.05 mmol), 0.5 mol% catalyst and 10 mol% K_2CO_3 in toluene (1.0 mL) at room temperature. [b] Determined by ^{1}H NMR spectroscopy. [c] Enantiomeric excesses and diastereomeric ratios were determined by SFC analysis. [d] 0.2 mol% catalyst was used. [e] N.D.: not determined.

and enantioselectivity. Notably, high levels of d.r. and *ee* were obtained in these cases where the starting substrate was fully converted to the mono-hydrogenated product (Table 1, entries 1, 3, 6). This experimental observation was found to be in good agreement with the mathematical model developed by Schreiber et al. that illustrates the enhanced levels of *ee* and d.r. obtained in a class of reactions that proceed with a combination of enantiotopic group and diastereotopic face selectivity.[12] In order to compare the initial selectivity of catalyst **A** and **C**, the hydrogenations were performed at lower hydrogen pressure (Table 1, entries 7, 8). In these cases, catalyst **C** showed higher selectivity than catalyst **A**. Finally, the best result was achieved by using catalyst **C** under 1 bar

hydrogen for 10 minutes, where the desymmetrized product **2a** was obtained in 95% NMR yield with perfect d.r. and *ee*.

With the optimized conditions in hand, we then examined the scope of this iridium-catalyzed desymmetric hydrogenation of divinylcarbinols (Table 2). Generally, the aromatic substrates bearing either an electron-donating or electron-withdrawing group in the *para* or *meta* position of the phenyl ring underwent the desymmetrization with excellent diastereoselectivities and enantioseletivities as well as isolated yields (**2a**–**2g**). Substrates bearing naphthyl, furyl, and thienyl moieties were also well tolerated, and the desired products (**2h**–**2j**) were obtained in high yields with excellent selectivities.

Next, divinyl carbinols with longer aliphatic sidechains in the alpha position were tested and the corresponding mono-hydrogenated products could be obtained with excellent selectivities (**2k**, **2l**). Remarkably, the divinyl tertiary alcohols smoothly underwent the desymmetrization to afford the target products (**2m**–**2o**) in high yields with very high diastereoselectivies and enantioselectivities. This is noteworthy since the resulting tertiary chiral centers are not accessible via direct asymmetric hydrogenations, and the current strategy represents a complementary method to the classical asymmetric vinylation of ketones to prepare enantioenriched trisubstituted allylic tertiary alcohols.[13]

Finally, a series of divinyl carbinols having only aliphatic substituents were also evaluated. Overall, substrates having linear, branched, or cyclic alkyl substituents in the beta position were all applicable, good to excellent yields and high level of selectivities were obtained in these cases (**2p**–**2t**). The absolute configuration of alcohol product **2p** was determined by oxidative cleavage of the olefin and comparison of the hydroxy ketone with an isoleucine derivative (see the SI for details). In addition, substrates bearing highly strained cyclopropyl (**2u**) and cyclobutyl (**2v**) underwent the desired desymmetrization smoothly without any traces of ring-opening via hydrogenolysis. Interestingly, other functionalities such as phenyl (**2w**), chloride (**2x**), and silyl ether (**2y**) were also compatible with the very mild hydrogenation conditions. A substrate containing cyclohexene moieties was also tested, the desired enantiomerically pure product (**2z**) was produced in 96% yield.

Given the success of the current desymmetrization of divinyl carbinols outlined above, we then decided to explore the desymmetric hydrogenation of divinyl carbinamine derivatives (Table 3), which are a new class of substrates for hydrogenative desymmetrization. To our delight, the Boc-protected divinyl carbinamines underwent the desired desymmetrization smoothy employing the same Ir catalyst. Notably, no base additive was requried for this transformation. Both electron-withdrawing and electron-donating groups on the phenyl ring were tolerated (**4a**–**4c**). Significantly, a series of aliphatic substrates were processed to give the corresponding mono-hydrogenated products (**4d**–**4h**) in high yields and excellent diastereoselectivities and enantioselectivities. The absolute configuration of product **4d** was assigned as (*4S*,*5S*) by comparing its ozonolysis product with a natural isoleucine derivative (see the SI for details).

Considering the unusually high level of *ee* and d.r. of the desymmetrized products as well as the very broad substrate scope that is obtained with the current method, DFT calculations were performed to investigate the stereoselectivity of the desymmetrization process. Divinyl carbinol **1a** was chosen as the model substrate and catalyst *ent*-**C** was employed in the studies. Based on our previous theoretical

Table 2: Scope of divinyl carbinol.[a]

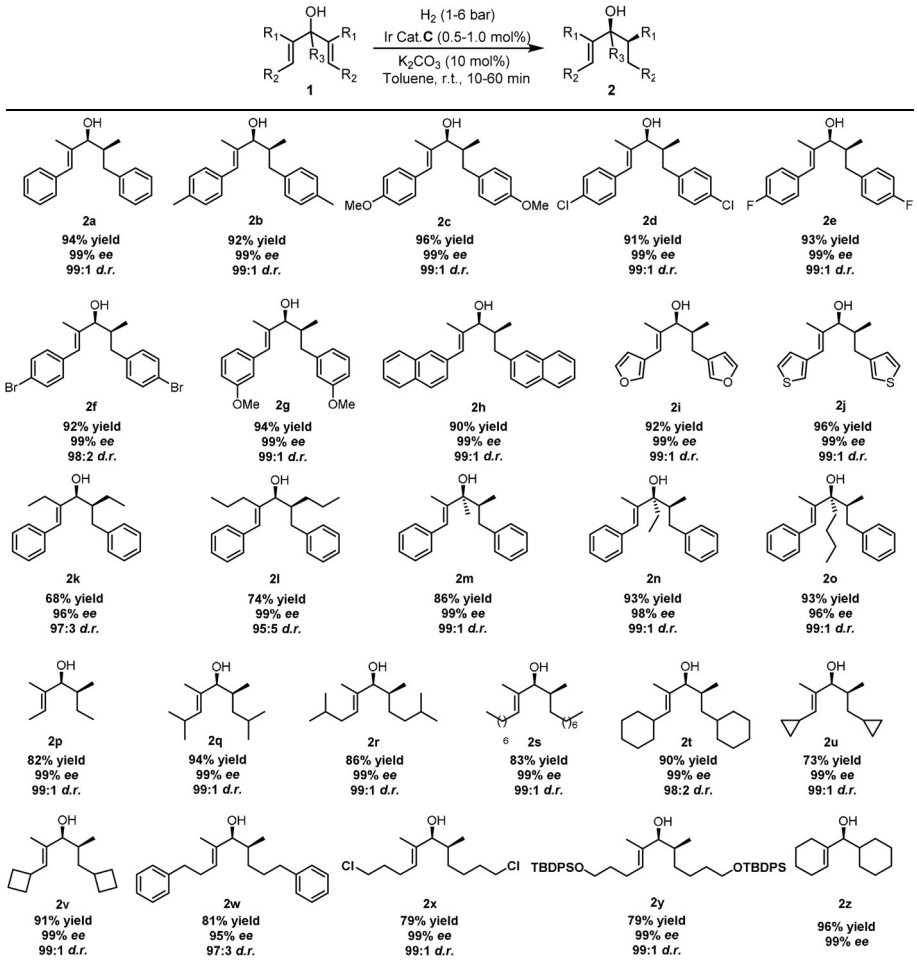

[a] Reaction conditions: substrate (0.2 mmol), 0.5–1.0 mol% catalyst, and 10 mol% K_2CO_3 in toluene (1.0 mL) under 1–6 bar H_2 at room temperature for 10 min–1 h. Isolated yield. Enantiomeric excesses and diastereomeric ratios were determined by SFC or GC analysis (see the SI for details).

Table 3: Scope of divinyl carbinamide.[a]

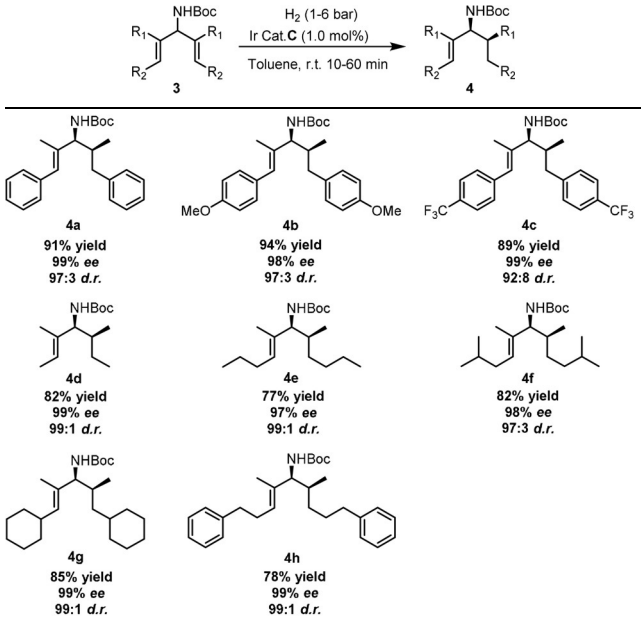

[a] Reaction conditions: substrate (0.2 mmol), 1.0 mol% catalyst, and 10 mol% K_2CO_3 in toluene (1.0 mL) under 1–6 bar H_2 at room temperature for 10 min–1 h. Isolated yield. Enantiomeric excesses and diastereomeric ratios were determined by SFC or GC analysis (see SI for details).

and experimental investigations on Ir-catalyzed asymmetric hydrogenation of olefins,[14] a mechanism of desymmetric hydrogenation is proposed (Figure 3). The computational details and the process of searching for the most stable substrate-catalyst complex are outlined in the Supporting Information (SI).

Since the studied *meso* compound has two enantiotopic and two diastereotopic faces, all four individual coordination models of both the first and the second hydrogenation (Scheme 1) were tested. The calculated free energies of four different intermediates and the corresponding olefin insertion transition states of the first hydrogenation are shown in Figure 4a. The following reductive elimination steps were confirmed to have lower free energies than the olefin insertions in all cases (SI, Figure S4).

The results indicate that product **2a(1_1)** will be the major product of the first hydrogenation but that significant

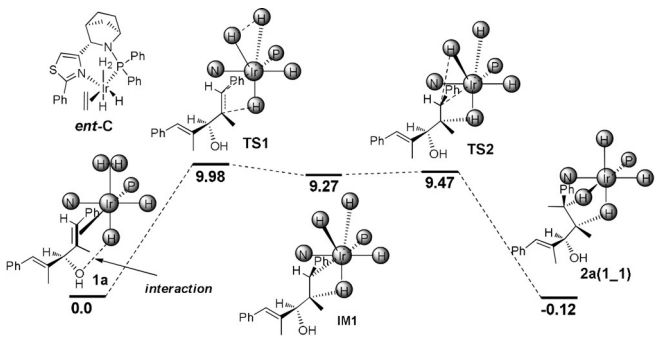

Figure 3. Proposed hydrogenation mechanism.

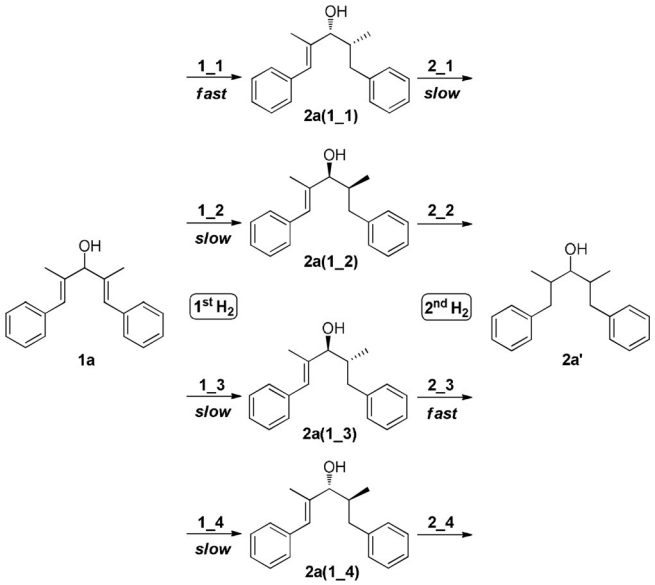

Scheme 1. Hydrogenative desymmetrization process.

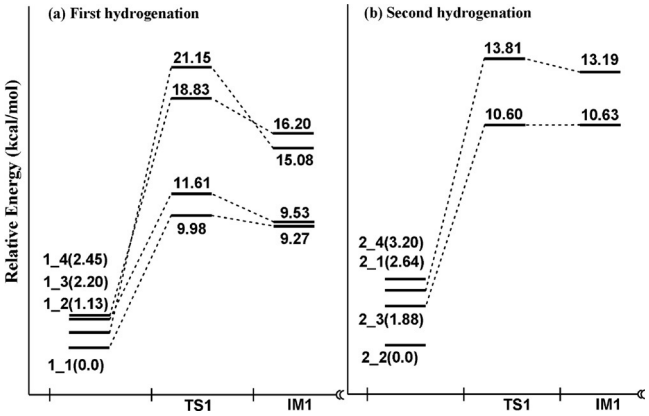

Figure 4. Free energy profile for a) the first hydrogenation; b) the second hydrogenation.

amounts of **2a(1_3)** will also form. The free energy difference between **TS1(1_1)** and **TS1(1_3)** is 1.63 kcal mol^{-1}, which suggested that over 90% diastereoselectivity could be observed in this step. Due to the much slower formation of **2a(1_2)** and **2a(1_4)**, here we only discuss the second hydrogenation of **2a(1_1)** and **2a(1_3)** as shown in Figure 4b (complete reactions are shown in SI, Figure S5). We found that the activation free energy for the reaction of the minor mono-hydrogenated product **2a(1_3)** via **TS1(2_3)** is very low, which will lead to a rapid consumption of **2a(1_3)**. The hydrogenation of **2a(1_1)** is significantly slower and will therefore be close to the only remaining singly hydrogenated olefin after some time. All of the predictions from DFT are consistent with the experimental results. The calculated free-energy profiles reveal that the hydrogenation of **2a(1_2)** and **2a(1_4)** is slow due to high activation free energies for the olefin insertion. By examining the structures, it is clear that **2a(1_2)** and **2a(1_4)** have an unfavorable substrate–complex configuration with the olefin double bond oriented in the

plane of the bidentate ligand (SI, Figure S3), instead of the orientation along the axial Ir–H bond in **2a(1_1)** and **2a(1_3)**. In all favorable insertion transition states (**TS1(1_1)**, **TS1-(1_3)** (SI, Figure S7) and **TS1(2_2)**, **TS1(2_3)** (SI, Figure S8) we found some interaction between the hydroxy oxygen atom and the reacting hydride, evidenced by O_1—H_a distances smaller than the sum of the van der Waals radii.

Using rate constants calculated using transition state theory (assuming a transmission coefficient of 1) with the calculated activation free energies, we have simulated the product distribution over time to give a more intuitive demonstration of the kinetics of the studied process.[15] As shown in Figure 5, in the early stage of the reaction, mono-hydrogenated product **2a(1_1)** increases very fast and is accompanied by the generation of a small portion of **2a(1_3)**, which is present as a minor diastereomer in the mixture. As the hydrogenation proceeds, the amount of **2a(1_1)** remains at a high level, however, the minor diastereomer or enantiomer will be selectivity consumed by a kinetic resolution process in the second hydrogenation. As a result, excellent levels of *ee* and d.r. were obtained in the current desymmetrization process. Notably, the current model could be also applied in a generic class of reactions that proceed with a combination of enantiotopic group and diastereotopic face selectivity.

In order to demonstrate the utility of the transformation, we synthesized the side chain fragment of natural product zaragozic acid A with this desymmetrization as a key step (Scheme 2). Firstly, a gram scale hydrogenation was performed, and the desired optically pure product **2a** was obtained in an undiminished yield. Then, ozonolysis of the resulting product afforded the hydroxy ketone **5**, which underwent bromoform reaction and condensation to give Weinreb amide **6** in 83% overall yield. Next, the inversion of alcohol was achieved using a Mitsunobu protocol. Finally, the PMB protection followed by alkylation furnished the target molecule **9** with 99% *ee*. Compound **9** is the enantiomer of

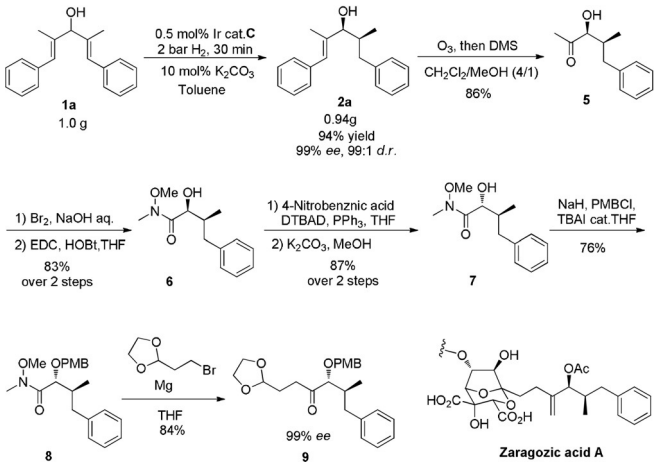

Scheme 2. Gram scale desymmetrization and application in the synthesis of the alkyl side chain fragment of zaragozic acid A.

Nicolaou's intermediate, which was initially synthesized in 12 steps with 81% *ee*.[16]

To further illustrate the usefulness of this methodology, we continued to explore its potential in the synthesis of γ-butyrolactones (Scheme 3), which are important structural units of a wide range of pharmacologically active molecules.[17] Ozonolysis of the desymmetrized product of **10** followed by hydroxy-directed Wittig reaction[18] afforded the unsaturated ester (*4S,5S*)-**12** as a single isomer with excellent d.r. and *ee* in 64% overall yield. Surprisingly, the obtained γ-hydroxy unsaturated ester can be transformed into lactone (*1′S,4R,5S*)-**13** directly under hydrogenation conditions with *ent*-**C** as the catalyst. We speculate that the γ-butyrolactone formation could be attributed to the acidic environment generated during the iridium-catalyzed hydrogenation.[19] Meanwhile, the inversion of the hydroxy group on (*4S,5S*)-**12** using a Mitsunobu protocol provided another diastereomer of unsaturated ester (*4R,5S*)-**12**. Similarly, one-pot

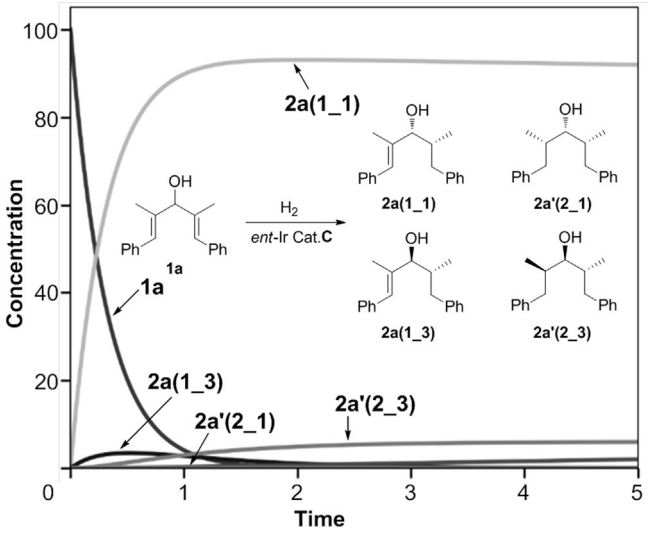

Figure 5. Kinetic modeling based on the calculated energy. Concentration in percent of total reactant and product concentration and time in 10^{-5} seconds.

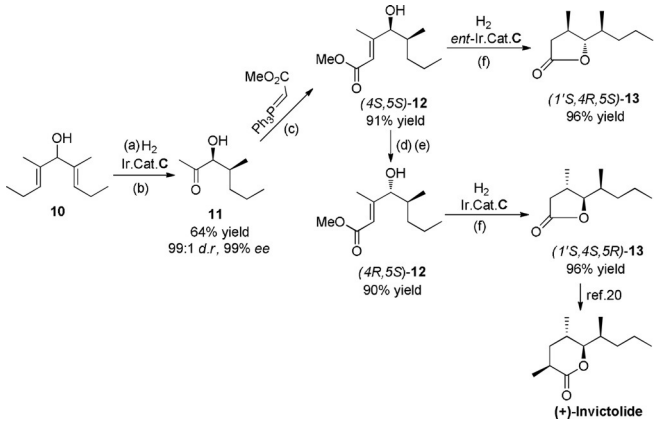

Scheme 3. Synthesis of γ-butyrolactones via a sequential desymmetrization and tandem hydrogenation and lactonization process: Formal total synthesis of (+)-invictolide. Reaction conditions: a) 0.5 mol% Ir cat., 10 mol% K_2CO_3, 3 bar H_2, toluene, r.t. 30 min; b) O_3, then DMS, CH_2Cl_2/MeOH 4:1; c) benzene, reflux, 24 h; d) 4-nitrobenzoic acid, DTBAD, PPh_3, THF; e) K_2CO_3, MeOH, r.t., 1 h; f) 1.0 mol% Ir cat., 3 bar H_2, toluene, r.t. 1 h.

hydrogenation and lactonization of (*4R*,*5S*)-**12** using catalyst **C** led to another diastereomer of γ-butyrolactone (*1'S*,*4S*,*5R*)-**13**, which is a known intermediate in the total synthesis of natural product (+)-invictolide.[20]

Conclusion

A highly efficient Ir-catalyzed site-selective desymmetric mono-hydrogenation of 1,4-dienes has been developed. This method provides a concise route to chiral allylic alcohols and allylic amides bearing two vicinal stereogenic centers adjacent to the alkene. It demonstrates the first Ir-catalyzed hydrogenative desymmetrization of dienes. Impressive regio-, diastereo-, and enantioselectivities (up to 96% yield, 99:1 d.r. and 99% *ee*) were obtained for a broad range of divinyl carbinol (secondary and tertiary alcohols) and divinyl carbinamide substrates. DFT calculations indicate that an interaction between the hydroxy oxygen atom and active Ir-hydride is most likely responsible for the stereoselectivities. Modeling based on the calculated energy profiles was applied to give an intuitive picture of the reaction kinetics, which could be also applied for a class of desymmetrizations with enhanced diastereo- and enantioselectivities. The utility of this method was further highlighted by the synthesis of the alkyl side chain of zaragozic acid A and the formal total synthesis of (+)-invictolide.

Acknowledgements

The authors are grateful to the Swedish Research Council (VR), the Knut och Alice Wallenberg Stiftelsen for funding this research. T.S. acknowledges the NRF South Africa for the Post-PhD Track Thuthuka Grant. All calculations were performed on resources provided by the Swedish National Infrastructure for Computing (SNIC) at PDC Centre for High Performance Computing (PDC-HPC) through the project "Small molecule activation by transition metals in complex environments" SNIC 2020/6-47, and the National Supercomputing Center under the project numbers SNIC 2019/3-6 and SNIC 2020/6-47 in Linköping, Sweden. M.S.G.A. is supported by the Swedish Research Council (VR) Grant Number 2018-05396, and the Knut & Alice Wallenberg (KAW) project CATSS (KAW 2016.0072).

Conflict of Interest

The authors declare no conflict of interest.

Keywords: 1,4-diene · asymmetric hydrogenation · iridium catalysis · site selectivity

[1] For a recent book, see: a) *Asymmetric Hydrogenation and Transfer Hydrogenation*, (Eds.: V. Ratovelomanana-Vidal, P. Phansavath), Wiley-VCH, Weinheim, **2021**; For some reviews see, b) W. S. Knowles, *Angew. Chem. Int. Ed.* **2002**, *41*, 1998–2007; *Angew. Chem.* **2002**, *114*, 2096–2107; c) R. Noyori, *Angew. Chem. Int. Ed.* **2002**, *41*, 2008–2022; *Angew. Chem.* **2002**, *114*, 2108–2123; d) D. J. Ager, A. H. M. de Vries, J. G. de Vries, *Chem. Soc. Rev.* **2012**, *41*, 3340–3380; e) C. S. Shultz, S. W. Krska, *Acc. Chem. Res.* **2007**, *40*, 1320–1326; f) N. B. Johnson, I. C. Lennon, P. H. Moran, J. A. Ramsden, *Acc. Chem. Res.* **2007**, *40*, 1291–1299; g) P. D. Parker, X. Hou, V. M. Dong, *J. Am. Chem. Soc.* **2021**, *143*, 6724–6745.

[2] For some reviews, see: a) D. C. Silva Costa, *Arab. J. Chem.* **2020**, *13*, 799–834; b) X.-W. Lan, N.-X. Wang, Y. Xing, *Eur. J. Org. Chem.* **2017**, 5821–5851; c) H. Jiang, A. Studer, *Chem. Soc. Rev.* **2020**, *49*, 1790–1811; d) G. Yin, X. Mu, G. Liu, *Acc. Chem. Res.* **2016**, *49*, 2413–2423; e) M. Beller, J. Seayad, A. Tillack, H. Jiao, *Angew. Chem. Int. Ed.* **2004**, *43*, 3368–3398; *Angew. Chem.* **2004**, *116*, 3448–3479; f) R. I. McDonald, G. Liu, S. S. Stahl, *Chem. Rev.* **2011**, *111*, 2981–3019; g) Z. Liu, Y. Gao, T. Zeng, K. M. Engle, *Isr. J. Chem.* **2020**, *60*, 219–229.

[3] For a review on site-selective control reactions, see: a) Z. Huang, G. Dong, *Acc. Chem. Res.* **2017**, *50*, 465–471; For some selected examples of site selective reaction of dienes or polyenes, see: b) P. A. Lichtor, S. J. Miller, *Nat. Chem.* **2012**, *4*, 990–995; c) C. Desfeux, C. Besnard, C. Mazet, *Org. Lett.* **2020**, *22*, 8181–8187; For a review, see d) C. Margarita, W. Rabten, P. G. Andersson, *Chem. Eur. J.* **2018**, *24*, 8022–8028; For some selected examples of regioselective asymmetric hydrogenation, see: e) H. Takaya, T. Ohta, N. Sayo, H. Kumobayashi, S. Akutagawa, S. Inoue, I. Kasahara, R. Noyori, *J. Am. Chem. Soc.* **1987**, *109*, 1596–1597; f) D. Valentine, K. K. Johnson, W. Priester, R. C. Sun, K. Toth, G. Saucy, *J. Org. Chem.* **1980**, *45*, 3698–3703; g) M. J. Burk, J. G. Allen, W. F. Kiesman, *J. Am. Chem. Soc.* **1998**, *120*, 657–663; h) J. Liu, S. Krajangsri, T. Singh, G. De Seriis, N. Chumnanvej, H. Wu, P. G. Andersson, *J. Am. Chem. Soc.* **2017**, *139*, 14470–14475; i) H. Wu, C. Margarita, J. Jongcharoenkamol, M. D. Nolan, T. Singh, P. G. Andersson, *Chem. Sci.* **2021**, *12*, 1937–1943.

[4] For some reviews, see: a) T. Ayad, P. Phansavath, V. Ratovelomanana-Vidal, *Chem. Rec.* **2016**, *16*, 2754–2771; b) X. Cui, K. Burgess, *Chem. Rev.* **2005**, *105*, 3272–3296; c) W. Tang, X. Zhang, *Chem. Rev.* **2003**, *103*, 3029–3070; d) W. Zhang, Y. Chi, X. Zhang, *Acc. Chem. Res.* **2007**, *40*, 1278–1290; e) P. Etayo, A. Vidal-Ferran, *Chem. Soc. Rev.* **2013**, *42*, 728–754; f) Q.-A. Chen, Z.-S. Ye, Y. Duan, Y.-G. Zhou, *Chem. Soc. Rev.* **2013**, *42*, 497–511; g) J. J. Verendel, O. Pàmies, M. Diéguez, P. G. Andersson, *Chem. Rev.* **2014**, *114*, 2130–2169; h) Z. Zhang, N. A. Butt, W. Zhang, *Chem. Rev.* **2016**, *116*, 14769–14827; i) C. S. G. Seo, R. H. Morris, *Organometallics* **2019**, *38*, 47–65.

[5] For some reviews, see: a) S.-F. Zhu, Q.-L. Zhou, *Acc. Chem. Res.* **2017**, *50*, 988–1001; b) S. J. Roseblade, A. Pfaltz, *Acc. Chem. Res.* **2007**, *40*, 1402–1411; c) C. Margarita, P. G. Andersson, *J. Am. Chem. Soc.* **2017**, *139*, 1346–1356.

[6] a) J. Merad, M. Candy, J.-M. Pons, C. Bressy, *Synthesis* **2017**, *49*, 1938–1954; b) H. Fernández-Pérez, P. Etayo, J. R. Lao, J. L. Núñez-Rico, A. Vidal-Ferran, *Chem. Commun.* **2013**, *49*, 10666–10675.

[7] B. Nguyen, J. M. Brown, *Adv. Synth. Catal.* **2009**, *351*, 1333–1343.

[8] H. Fernández-Pérez, J. R. Lao, A. Vidal-Ferran, *Org. Lett.* **2016**, *18*, 2836–2839.

[9] C. You, X. Li, Q. Gong, J. Wen, X. Zhang, *J. Am. Chem. Soc.* **2019**, *141*, 14560–14564. A number of leading examples of catalytic desymmetrization of cyclohexadienones are cited herein.

[10] a) J. D. Bergstrom, M. M. Kurtz, D. J. Rew, A. M. Amend, J. D. Karkas, R. G. Bostedor, V. S. Bansal, C. Dufresne, F. L. VanMiddlesworth, O. D. Hensens, *Proc. Natl. Acad. Sci. USA* **1993**, *90*, 80–84; b) R. W. Burg, B. M. Miller, E. E. Baker, J. Birnbaum, S. A. Currie, R. Hartman, Y.-L. Kong, R. L. Monaghan, G. Olson, I. Putter, J. B. Tunac, H. Wallick, E. O. Stapley, R.

Oiwa, S. Ōmura, *Antimicrob. Agents Chemother.* **1979**, *15*, 361 – 367.
[11] a) A. Paptchikhine, K. Itto, P. G. Andersson, *Chem. Commun.* **2011**, *47*, 3989 – 3991; b) B. K. Peters, J. Liu, C. Margarita, W. Rabten, S. Kerdphon, A. Orebom, T. Morsch, P. G. Andersson, *J. Am. Chem. Soc.* **2016**, *138*, 11930 – 11935; c) J. Liu, S. Krajangsri, J. Yang, J.-Q. Li, P. G. Andersson, *Nat. Catal.* **2018**, *1*, 438 – 443; d) W. Rabten, C. Margarita, L. Eriksson, P. G. Andersson, *Chem. Eur. J.* **2018**, *24*, 1681 – 1685; e) J. Zheng, C. Margarita, S. Krajangsri, P. G. Andersson, *Org. Lett.* **2018**, *20*, 5676 – 5679; f) S. Krajangsri, H. Wu, J. Liu, W. Rabten, T. Singh, P. G. Andersson, *Chem. Sci.* **2019**, *10*, 3649 – 3653.
[12] S. L. Schreiber, T. S. Schreiber, D. B. Smith, *J. Am. Chem. Soc.* **1987**, *109*, 1525 – 1529.
[13] H. Li, P. J. Walsh, *J. Am. Chem. Soc.* **2005**, *127*, 8355 – 8361.
[14] T. L. Church, T. Rasmussen, P. G. Andersson, *Organometallics* **2010**, *29*, 6769 – 6781.
[15] We note that the reaction time is shorter than in the experiment, likely due to formation of common low energy intermediates that do not directly lead to product. Such intermediate would slow down all reaction equally. For program information, see: K. A. Johnson, Z. B. Simpson, T. Blom, *Anal. Biochem.* **2009**, *387*, 20 – 29.
[16] a) K. C. Nicolaou, E. W. Yue, Y. Naniwa, F. De Riccardis, A. Nadin, J. E. Leresche, S. La Greca, Z. Yang, *Angew. Chem. Int. Ed. Engl.* **1994**, *33*, 2184 – 2187; *Angew. Chem.* **1994**, *106*, 2306 – 2309; b) K. C. Nicolaou, E. W. Yue, S. la Greca, A. Nadin, Z. Yang, J. E. Leresche, T. Tsuri, Y. Naniwa, F. de Riccardis, *Chem. Eur. J.* **1995**, *1*, 467 – 494.
[17] a) S. Singha, E. Serrano, S. Mondal, C. G. Daniliuc, F. Glorius, *Nat. Catal.* **2020**, *3*, 48 – 54; b) B. Mao, M. Fañanás-Mastral, B. L. Feringa, *Chem. Rev.* **2017**, *117*, 10502 – 10566.
[18] P. Garner, S. Ramakanth, *J. Org. Chem.* **1987**, *52*, 2629 – 2631.
[19] a) R. G. Pearson, *Chem. Rev.* **1985**, *85*, 41 – 49; b) Y. Zhu, Y. Fan, K. Burgess, *J. Am. Chem. Soc.* **2010**, *132*, 6249 – 6253.
[20] a) F. E. Ziegler, W. T. Cain, A. Kneisley, E. P. Stirchak, R. T. Wester, *J. Am. Chem. Soc.* **1988**, *110*, 5442 – 5452; b) T. Honda, S.-i. Yamane, F. Ishikawa, M. Katoh, *Tetrahedron* **1996**, *52*, 12177 – 12184.

Manuscript received: May 31, 2021
Accepted manuscript online: June 17, 2021
Version of record online: July 20, 2021

